Scientia Iranica B (2015) 22(5), 1855–1865

Sharif University of Technology
Scientia Iranica
Transactions B: Mechanical Engineering
www.scientiairanica.com

Analysis, modeling, manufacturing and control of an elastic actuator for rehabilitation robots

M.D. Hasankola[a], A. Ehsaniseresht[b], M.M. Moghaddam[a,*] and A.A. Mirzaei Saba[a]

a. *Department of Mechanical Engineering, Tarbiat Modares University, Tehran, Iran.*
b. *Department of Mechanical Engineering Hakim Sabzevari University, Sabzevar, Iran.*

Received 22 May 2014; received in revised form 29 November 2014; accepted 16 June 2015

KEYWORDS
Elastic actuator;
Bandwidth;
Rehabilitation;
Impedance control.

Abstract. In this paper, modelling and control of an elastic actuator for rehabilitation robots are investigated. First, the required performance of the actuator is determined, and then a model of the actuator is proposed. Further, a control algorithm is presented to meet the required performance specifications. The control algorithm consists of an external PID torque controller and an internal PI speed Controller. Experimental tests are performed on the actuator to evaluate the actuator performance. First, an accuracy evaluation test is performed on the actuator to calibrate the torque measured by the spring. The results exhibit the spring's linear characteristics and the capability of torque measurement. Second, the bandwidth of the actuator is measured through sinusoidal input. The results show that the actuator is capable of delivering the required torque in the frequency range of rehabilitation. Third, an impedance measurement test is performed on the actuator indicating that it is capable of exerting the lowest and/or highest resistance on patient movement if required. As a result, it is shown that the proposed actuator can satisfy the whole rehabilitation requirements appropriately.

1. Introduction

To restore the movement capability of stroke patients, one should exert repeated exercises to the damaged body members of the patients. These exercises were performed manually on the patient in common. However, the human beings were gradually replaced by the rehabilitation robots because of the fact that the robots can transfer the appropriate movement patterns with no exhaustion and relaxation to the patients. One of the most significant rehabilitation requirements is performing the movement patterns due to the provision of the required torque for the movement of the members of patient's body. Regardless of the amount of the torque, the bandwidth of the rehabilitation robot is also very significant, as it should correspond to the movement frequency of human being. Also, the required torque should also be delivered by the robot for rehabilitation. In order to achieve an appropriate force control, an elastic element can be used between the load and the motor. The elastic actuator has accompanied a specific design which is different from the design of conventional actuators. In the elastic actuator, a soft interface is used between the actuator and the load. Also a position sensor is used in the elastic actuator which, by measuring the position, can help along with the Hook's relation to calculate the resultant output force. The elastic actuators have a lot of advantages for robotic applications such as generation capability of high force, low resistance in output, appropriate force bandwidth [1].

So far, various actuators have been presented for rehabilitation applications such that each has advan-

*. *Corresponding author. Tel.: +98 21 82883358; Fax: +98 21 88005040*
E-mail address: m.moghadam@modares.ac.ir (M.M. Moghaddam)

tages and disadvantages. One type of these actuators is direct drive electric actuators. These actuators use a heavy electric motor which has the ability to generate high torques, and is directly connected to the load. Due to heaviness, they often have industrial applications. The pneumatic actuators are also used in rehabilitation applications. In pneumatic actuators, the force is controlled by controlling pressure. In these actuators, the friction prevents the generation of low forces. Also, because the air in pneumatic actuators is compressible, its position is very difficult. Another type of actuators, which has been used a lot, is the electric actuators with a gear system. These actuators use a gear system to increase the capability of torque generation due to which the effects of friction and inertia on the output increase. The reflected inertia in output side increases with factor 2 of the gear ratio. In this type of actuator, a control loop and a force gauge are used to control the torque. The force gauge, which is directly connected to the load, bears various disadvantages in its use. The use of load-cell can cause stability problems. In situations where the load-cell is positioned between linear operator and rigid load, even a small linear displacement of the actuator causes a large force in the load-cell. In order to resolve the problems associated with the introduced actuators, series elastic actuators are recommended. In Figure 1, the schematic of a series elastic actuator is used [2].

The elastic actuators are a type of low-pass filters. The elastic actuators convert the force control to the position control. This behavior considerably increases the accuracy of the force control. In the elastic actuator, the amount of spring displacement is obtained by using the position sensor, and the Hook's law is used to obtain the force. The reason that the position control is more appropriate than the force control is that, using a series of gears, the position is controlled much simpler than force. Finally, the elastic actuator provides the possibility of energy-saving. In foot motion the energy-saving causes the increase of efficiency. In series elastic actuators, the load-cell (which is sensitive and expensive, and causes impact and instability) is substituted with an elastic force gauge (which is more resistant, cheaper and more stable) [3].

The goal of the present paper is to offer the design of an elastic actuator for knee joint of a rehabilitation robot. In the present paper, first the requirements of the rehabilitation applications are investigated, and a model of the actuator is presented. Then, the design of the actuator is investigated, the actuator is modelled in whole, and the torque control is applied on the actuator. Finally, the required tests are performed on the actuator to determine the performance of the actuator. By the use of an appropriate control loop, the actuator suitably provides the rehabilitation requirements mentioned above, and is applicable in rehabilitation robots. It should be mentioned that this elastic actuator is used in the rehabilitation robot of the "Tarbiat-Modarres University".

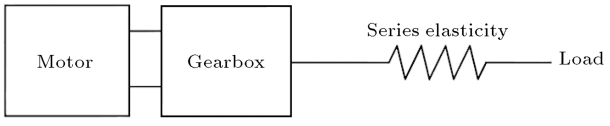

Figure 1. Schematic of the elastic actuator.

2. Modeling of the series elastic actuator

2.1. Input characteristics of the actuator system

Due to one analysis, Dollar et al. [3] wrote down the bio-mechanical values obtained for a 28 years-old healthy man with 82 kg weight and 99 cm feet length in a movement with velocity of 1.27 m/s. According to the obtained data, they calculated the joints angles, applied torque and consumed power in hip, knee and ankle joints. Figures 2 to 4 show the values obtained for lower extremity joints. In Figure 2, the required torque for the hip joint is shown. The maximum value of torque is 47 Nm which will be used in the next sections. The angles resulted from the movement of the knee joint are shown in Figure 3. The maximum angle variation for to the knee joint is 1 rad. Figure 4 shows the consumed power for joints which is 150 W for the knee joint.

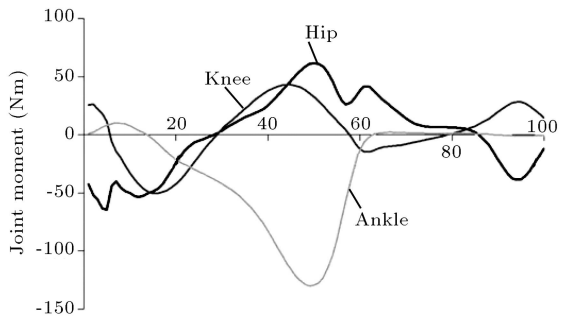

Figure 2. The consumed torque of joints in a gait cycle [3].

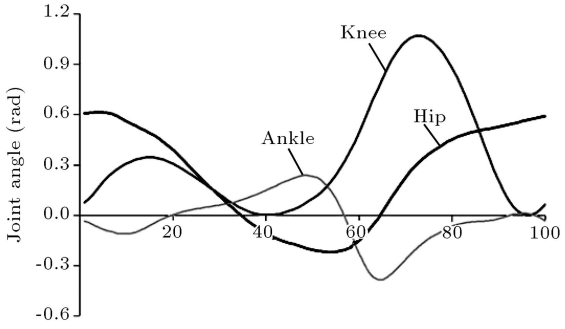

Figure 3. The angle variation of joints in a gait cycle [3].

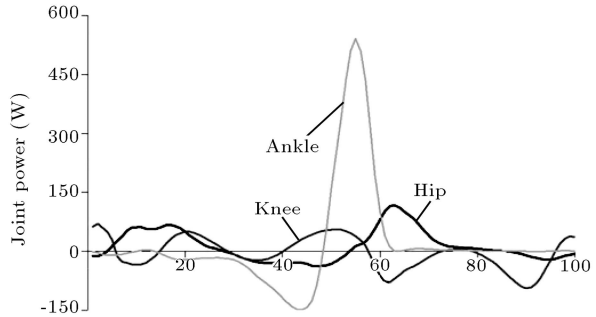

Figure 4. The consumed power of joints in a gait cycle [3].

Due to the fact that in rehabilitation applications, and particularly in rehabilitating robots, a part of patient's weight is supported by using some type of holders, the actuator endures only a part of patient's weight for moving the patient's body members. Therefore, the actuators used in these robots provide 50 to 60% of the torque required by the knee joint. If the actuator, designed in the next section, satisfies this condition, the actuator can be used in rehabilitation robots.

2.2. Modeling of the actuator

2.2.1. The overall model of the actuator

The actuators can transfer power in two ways: linear and rotational. Selection of each of these ways depends on their use in rehabilitation robots. Due to the design of the rehabilitation robot of the "Tarbiat-Modarres University" in which this actuator will be used, the rotational type of the actuator is selected.

Figure 5 shows the various parts of the actuator including motor, gearbox 1, torsional spring and gearbox 2.

2.2.2. Kinematic model of the actuator

The governing equations of the kinematic behavior of the actuator can be derived due to Figure 5. The governing equations of the system are as follows:

$$\theta_1 = \frac{\theta_m}{\eta_1}, \tag{1}$$

$$\theta_L = \frac{\theta_s}{\eta_2}, \tag{2}$$

$$\omega_1 = \frac{\omega_m}{\eta_1}, \tag{3}$$

$$\omega_L = \frac{\omega_s}{\eta_2}. \tag{4}$$

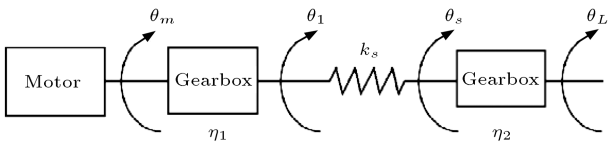

Figure 5. Overall schematics of the actuator.

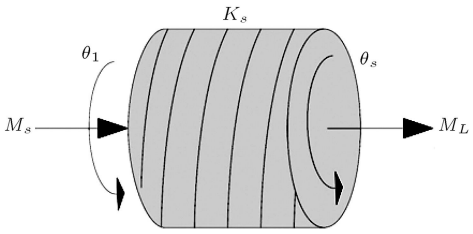

Figure 6. Free body diagram of the spring.

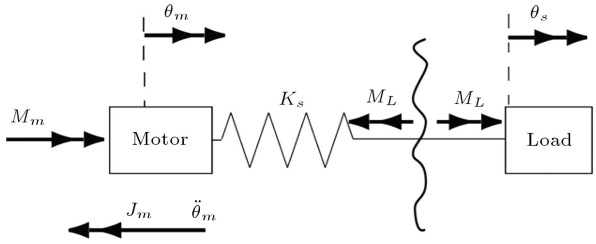

Figure 7. A model of the actuator without consideration of gear ratio.

2.2.3. Dynamic model

In Figure 6, the free-body diagram of the spring is shown by which the governing equations of the actuator can be derived. First, a model is considered in which a gear ratio is not included.

Due to Figure 7, the governing dynamic equation of the system is as follows:

$$M_L = K_s(\theta_m - \theta_s) \Rightarrow \theta_m = \frac{M_L}{K_s} + \theta_s, \tag{5}$$

$$J_m\ddot{\theta}_m = M_m - M_L. \tag{6}$$

According to Eqs. (5) and (6), the following can be written:

$$M_m = M_L + \frac{J_m}{K_s}s^2 M_L + J_m s^2\theta_s. \tag{7}$$

Now, if the modeled system has the gear ratio of η_1 between motor and spring and also η_2 between spring and load, the values of parameters vary, which are shown in Table 1. According to this table, Eq. (7) changes as follows:

Table 1. Calculations of the gear ratio.

With gear ratio	Without gear ratio
$\frac{M_L}{\eta_2}$	M_L
$M_m\eta_1$	M_m
$J_m\eta_1^2$	J_m
$\frac{\theta_m}{\eta_1}$	θ_m
$\theta_L\eta_2$	θ_s
$\frac{\omega_m}{\eta_1}$	ω_m
$\omega_L\eta_2$	ω_L

$$M_m\eta_1 = \frac{M_L}{\eta_2} + \frac{J_m\eta_1^2}{K_s}s^2\frac{M_L}{\eta_2} + J_m\eta_1^2\eta_2 s^2\theta_L, \quad (8)$$

$$M_s = M_m\eta_1, \quad (9)$$

$$M_L = M_s\eta_2, \quad (10)$$

$$M_L = M_m\eta_1\eta_2. \quad (11)$$

It is assumed that the actuator provides 50 to 60% of the patient's required torque. The reason for this assumption is that all the rehabilitation robots support a part of patient's weight by a support mechanism. This fact causes the actuators used in robots not to provide the whole torque required by the patient. As shown in Figure 2 and considering this assumption, the maximum rating torque in output for the knee joint is approximately 24 Nm. However, in order to be assured about the actuator ability to generate torques higher than 24 Nm, the maximum nominal torque in output for the knee joint is considered to be 34 Nm. Now, with the values of the torque and angular velocity, and using Eq. (11), the required gear ratios can be obtained.

2.2.4. Choosing the actuator components

2.2.4.1. Gearbox

By Eq. (11) and Table 2 the following are obtained:

$$M_L = M_s\eta_2 = M_m\eta_1\eta_2 \Rightarrow 34 = 0.323\eta_1\eta_2,$$

$$106 = \eta_1\eta_2. \quad (12)$$

The gear ratio for the knee joint is obtained to be 17. It should be noted that this gear ratio is for $\eta_1\eta_2$ as shown in Figure 5. In the design of this actuator, the gear ratio is divided into two sections, which has the reasons as follows:

- The division of gear ratio into two sections and placing the spring between those two sections cause the spring to provide the required torque by having lower amount of rotation. This result causes the increase of performance velocity of the actuator and the increase of bandwidth. If we use both gears in motor side, the deflection of the spring increases and the bandwidth decreases. If we use both gears in load side, the deflection of the spring decreases and the bandwidth increases, so that we can not accurately measure the deflection of the spring in this case. So, we must find two proper ratios that at the same time give us bandwidth and accurate measuring;
- For using the actuator output in the knee joint of rehabilitation robot of "Tarbiat Modardes University", the rotational axis should be transferred to normal direction of the axis. To achieve this, a pair of bevel gears is used;
- The designed encoder works based on the angular difference of two ends of the spring. In order to read the position of one side of the spring, motor encoder is used. The position at other side of the spring is read by an encoder connected to a bevel gear.

Table 2. Motor specification.

Parameter	Values
Nominal voltage (V)	48
Nominal speed (rpm)	5770
Nominal torque (mNm)	323
Nominal current (A)	4.82
Inertia (gcm^2)	29

Accordingly, the conversion ratio is chosen as follows:

$$\eta_1 = 53, \quad \eta_2 = 2.$$

The bevel gear conversion ratio is $\eta_2 = 2$, the reason for this choice is that:

- Any increase in this conversion ratio causes the increase of the bevel gear size which is not favorable, because the bevel gear weight increases due to the iron material of the bevel gear;
- Increasing the gear ratio leads to the reduction of the amount of torque reaching to the spring end, which in turn causes a decrease in maximum torsion of the spring, and thus an increase in the measurement error.

2.2.4.2. Torsional spring

The spring constant can be chosen in 3 ways:

- High spring constant:
  In this case, the bandwidth of the actuator increases due to more rigidity of the system. However, decreasing the spring displacement makes measurement more difficult and with more error;
- Medium spring constant:
  This case is considered in design of spring. In this case, the actuator will have an appropriate bandwidth with less error;
- Low spring constant:
  In this case, the bandwidth considerably decreases. However, the measurement of the spring angular variation will be easier.

In the design of this actuator, the medium spring constant is considered. According to the relation of $T_s = K_s(\theta_M - \theta_L)$ and having the value of T_s, the spring constant can be obtained noting the value of $(\theta_M - \theta_L)$. To calculate the spring specification, the maximum spring displacement is assumed to be $(\theta_M - \theta_L) = 15$ deg (0.2618 rad) to achieve the required bandwidth

(at least 6 Hz) according to [5]. The value of spring constant equals $K_s = 65$ Nm/rad.

$$T_s = K_s(\theta_M - \theta_L) = \frac{T_L}{2} \Rightarrow 17 = K_S(0.2618),$$

$$K_s = 65. \tag{13}$$

3. Implementation of control algorithms and test of actuator

3.1. Methods used for control

The elastic actuators, due to their special mechanical design, require an appropriate control method. A much different architecture has been proposed for controlling series elastic actuators. Some of variations in controller design are rooted in differences imposed by the hardware. For example, force can be observed either by measuring change in resistance, as is accomplished using strain gauges in [1], or by measuring spring deflection and applying Hooke's law, as shown in [6]. Pratt and Williamson were the first who briefly expressed the advantages of elastic actuator. They offered a primitive control structure which adjusted the force by adjusting the current of a DC motor [6].

This structure contained a PID controller and several reverse dynamic expressions. All of these expressions are used for a few intensions, such as accelerating the motor inertia to follow the load movement and to deflect the spring, and approaching the required inertia at outlet. A control strategy for hardware designs, using spring deflection sensors, may treat a motor as a velocity source, and transform desired spring forces into desired spring deflections. However, for hardware designs using strain gauges, the force sensor does not output an intermediate displacement value, but maps a change in resistance directly to the applied force. For such a system, modeling the motor as a force source is more convenient. Further classification of SEA control strategies may be made based on the types and combinations of control structures used [5,7,8] to measure the spring force and control motor force using some subset of PID control structures (P, PD, etc.). If friction and backlash are too large, then a pure high-gain PID approach can suffer from stability issues. To remedy this issue, Pratt et al. [9] suggested using position feedback as the innermost control structure for force control. This idea has been adopted and carried on by many others, treating force control as a position tracking problem [10-12]. A new loop control has also been presented by Wyeth which, unlike the current loop of Pratt and Williamson, is based on the internal control loop of motor speed [13]. Another class of controllers uses PID control but consider the dynamics of the mechanical system to improve the frequency response of force control [1,14].

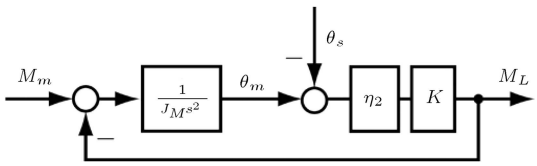

Figure 8. The actuator model.

3.2. Control method presented for the actuator

The control algorithm used for the actuator is such that it uses a speed feedback and PI controller for the motor control. In order to control the generated torque of the actuator, a PID controller is also used. The use of speed command instead of current command, in the DC motors, becomes attractive due to the fact that a velocity control loop on the motor can overcome some of the undesirable effects of the motor and the gearbox [13]. The speed in the actuator output is obtained by using the motor speed and the gear ratio. In this approach, the un-modeled torque resulting from the bevel gear friction is compensated by the quick loop of internal speed control. Also the special information of motor inertia is not needed. This control method causes the improvement of system performance.

3.2.1. Actuator model

In order to describe our model, we use Eqs. (5) and (6). The actuator model with gearboxes used in two sections of the actuator is shown in Figure 8. In -this model, the motor and gearbox are indicated as a complex with J_M which is equal to:

$$J_M = J_G + \eta_1^2 J_m, \tag{14}$$

$$\theta_m = \frac{\theta_m}{\eta_1}. \tag{15}$$

Here, two feedback loops and PI and PID controllers are used to control the actuator, which will be shown in the next sections.

3.2.2. Internal velocity control loop

When the advantages of this control approach are expressed, the motor will be seen as a generation source of speed rather than a generation source of torque. With this view, many of the previously mentioned disadvantages will be resolved. In this loop, the favorable speed input will be followed by using speed feedback loop. The motor does this work by providing the torque which makes this speed. In this control loop, a torque feedback is also used which indicates the amount of torque applied to motor. This feedback has only a theoretical basis because in reality this torque is automatically applied to motor by the mechanical connection of motor to load. A PI controller is used to correct the speed error in this loop. Figure 9 shows the schematic of the control loop used for motor control. As seen, the speed feedback is used for the motor control.

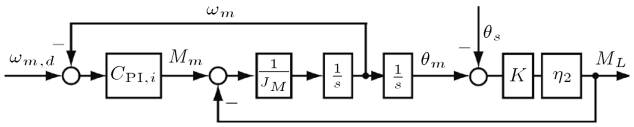

Figure 9. Schematics of motor control by speed feedback loop and the PI controller.

3.2.3. External torque control loop

Next, to follow the output torque by the actuator, output torque feedback and a controller are required. A PID controller is also used here to follow the output torque from the input torque. The control loop used is shown in Figure 10.

Noting the control loop shown in Figure 10, the relation between output torque and actuator input is expressed in Eq. (16).

$$\frac{M_L}{M_{L,d}} = \frac{2C_{\mathrm{PID}}C_{\mathrm{PI}}(\eta_2 K)}{J_M s^2 + C_{\mathrm{PI}} s + (1 + 2C_{\mathrm{PID}}C_{\mathrm{PI}})\eta_2 K}. \quad (16)$$

3.2.4. Impedance transfer function

The transfer function between the actuator output angle θ_L and the generated torque in output can also be written. This transfer function is the indicator of the system resistance Z in output.

$$Z = \frac{M_L}{-\varphi_L} = \frac{(\eta_2 K) J_M s^2}{J_M s^2 + C_{\mathrm{PI}} s + (1 + 2C_{\mathrm{PID}}C_{\mathrm{PI}})\eta_2 K}. \quad (17)$$

Eq. (17) shows that the transfer function Z of the system resistance in output has the two same poles of the transfer function M_L/M_{Ld}.

3.2.5. Controller design

Next, the coefficients of controllers are obtained by the stability optimization method of Zeigler-Nichols. The values obtained by using this method are shown in Table 3. Each of the control loops is separately investigated and the coefficients for each are determined.

According to the coefficients presented in Table 3, the Bode diagram for the closed-loop transfer function

Table 3. The theoretical control coefficients obtained by using the method of Zeigler-Nichols.

Control coefficients	
K_{po}	80
K_{io}	20
K_{do}	1
K_{pi}	20
K_{ii}	4

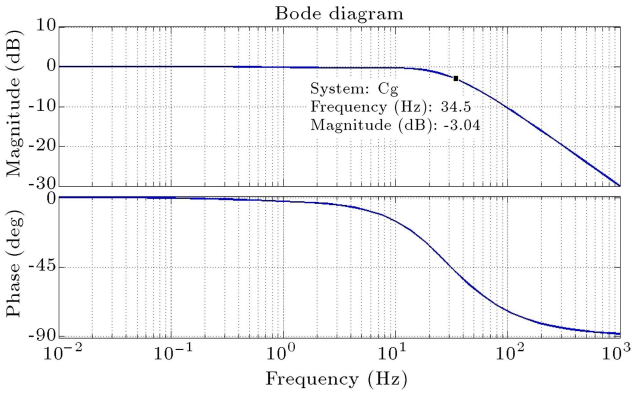

Figure 11. The Bode diagram of the closed-loop transfer function.

M_L/M_{Ld} can be plotted, which is shown in Figure 11. Due to this figure, the bandwidth obtained from the modeling is 34 Hz. In this modeling, which is performed in software MatLab, all the conditions and limitations of the motor are taken into account.

3.2.6. Achieving the required indexes to achieve

According to what was expressed in the previous sections, the favorite control algorithm should be implemented in the actuator, and then the various tests should be performed on the actuator. After the control loop is implemented in the actuator, a few indexes such as the followings are significant to be achieved:

1. The bandwidth required for rehabilitation applications;
2. The ability of torque control;
3. Lowering resistance at output by the use of loop control.

4. Test of actuator

4.1. Performance of favorite experiments on the actuator

To start-up the actuator and perform various tests on it, arbitrary control commands should be sent to the actuator motor, in order for the motor to provide the required torques at the output. To do this, the Maxon driver is used. The considered controls can be implemented on the actuator by the help of this driver. The tests performed on this actuator are the tests which have been performed on most of actuators presented so far. In other words, these tests have become the necessary standards of the actuators for

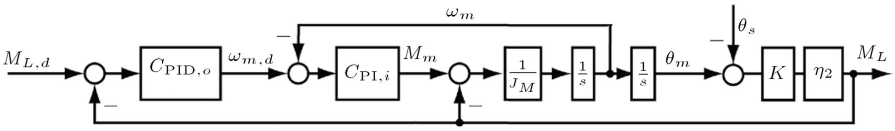

Figure 10. Schematic of the control loop for the actuator torque.

Table 4. The motors used in various actuators.

Actuator name	Motor used
RSEA	Maxon RE-25
CRSEA	Maxon RE-40
LOPES	Kolmorgen-Akm
LOKOMAT	Maxon Re-40
4DOF-RB	Maxon Re-40
ALEX	Maxon Re-40

rehabilitation applications and indicate the actuator performance. These tests include:

1. The accuracy test of torque measurement by the spring;
2. The measurement test of the force bandwidth;
3. The test of external impedance control.

4.2. Hardware used

In order to perform the intended tests on the actuators, a set of hardware for communicating with the actuator and a complex of computer codes for implementing the control algorithms are required. The motor used in this actuator is Maxon to which a 500 pulse encoder is also connected. The driver used in this actuator is called 50/5 epos which has the ability of position control and current control. A USB is used to connect this driver to a computer and to transport software commands from the computer to the driver. One of the driver ports is also used for reading the encoder [15]. Table 4 shows the motors used in various actuators.

4.3. Experiments required for performance evaluation of the system

4.3.1. Accuracy investigation of the torque measurement by spring

As it was mentioned previously, a spring in the actuator is used for torque measurement. This action is done by measuring the angle of two ends of the spring, such that the angle of one end is measured by a Hall sensor and the angle of the other end is measured by the encoder. By the use of angular difference of the two ends of the spring, and the substitution in Hook's law, it becomes clear that how the spring deflection causes the torque to be appeared at output. To test the accuracy of torque measurement by the spring, the actuator output is held constant (Figure 12). Then, as shown in Figure 12, a strain-gauge is placed between the actuator output (bevel gear) and the metallic arm. In this way, the resultant data of spring can be verified. Now, to perform this test, a steepness input is applied to the spring by the motor. By the use of strain-gauge, the value of angular strain generated at the output is measured. Using this value and the conversion relations of angular strain to torque, the resultant torque at the output is obtained. The obtained torque is then

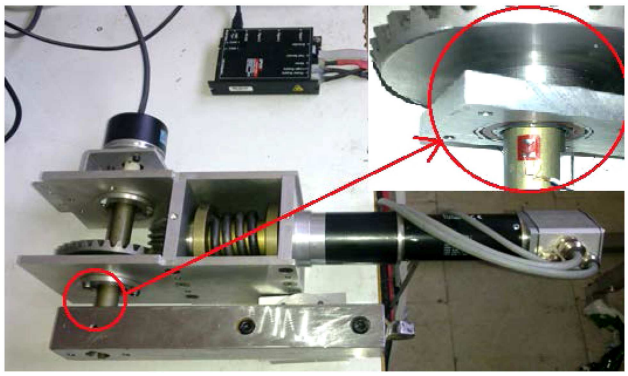

Figure 12. Series elastic actuator of knee joint for "Tarbiat Modares University" rehabilitation robot.

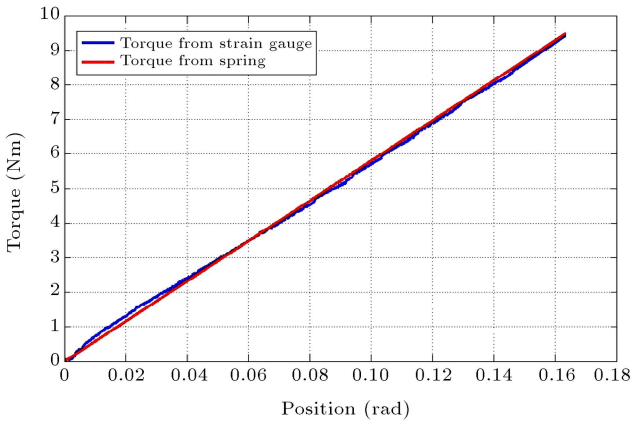

Figure 13. The diagram of torque variation in terms of the angle variation.

compared with the torque calculated by the Hook's law $T = K\Delta\theta$. The results of this test are shown in Figure 13.

In order to read the strain-gauge information in this test, first the strain-gauge is connected to strain-gauge information-writer set-up. Then the output of this set-up is connected to an analog input card. The analog output card is connected to a computer and is able to read the signals of the information-writer set-up. Thus the resultant data of the strain-gauge can be observed. The strain-gauge information-writer set-up indicates the amount of angular strain. The following relations are used to convert angular strain to torque.

$$\tau = G\gamma, \tag{18}$$

$$\tau = \mathrm{TC}/J, \tag{19}$$

$$J = \pi c^4/2. \tag{20}$$

The torque shown in Figure 13 is in the spring side, i.e. the torque generated at the output is two times of the torque at the spring side=19 Nm), which is adequate for indicating the spring linearity. As can be seen in Figure 13, the spring behaves more linearly with the

increase of torque. It should be mentioned that the results are obtained after several tests. The reason is to determine the realistic value of the spring constant which, after several tests, is obtained to be $K = 58$ Nm/rad. This value differs from the value obtained from theoretical calculation (i.e. $K = 65$ Nm/rad). As shown in Figure 13, an approximately linear torque is generated by the spring, which indicates the spring linearity. Thus, it can be concluded that the accuracy of torque measurement by the spring is appropriate and the spring can be used in the control loop.

4.3.2. Investigation of the bandwidth of force-following with constant output

In order to measure the bandwidth of the actuator, the actuator output is screwed to a table by a metallic arm (Figure 12). Then the torque outputs with various frequencies (from low to high frequencies), with the constant amplitude of 3 Nm, are applied as inputs to the actuator control loop. Now, control coefficients of PI and PID controllers are adjusted such that actuator could have the highest torque-following behavior. These control coefficients are shown in Table 5. Next, this torque is compared with the torque generated by the actuator. The result is the ratio of M_L/M_{Ld}. In a specific frequency, this ratio approaches to $M_L/M_{Ld} = 0.7$, that is the frequency of the actuator bandwidth. This action is done on the actuator and the results are shown in Figure 14. It can be seen in Figure 14 that the force bandwidth of the system is approximately 12 Hz. Noting the results obtained by the modeling and experiments, the obtained bandwidths are different for the two methods. By modeling, the bandwidth is 34 Hz but the bandwidth by the experiments is 12 Hz. One reason for this difference is that the actuator could not be completely modeled in the software. In modeling, many of the parameters available in reality cannot be added. Therefore, the obtained difference is reasonable because the actuator is constrained in the implementation and in the test. Due to the constancy of the actuator output for safety of experiment, the angular speed and angular acceleration of the motor are constrained. Thus the actuator is not damaged in the time of error appearance.

Table 5. The values of control coefficients.

Control coefficients	
K_{pi}	30
K_{ii}	10
K_{po}	50
K_{io}	10
K_{do}	2

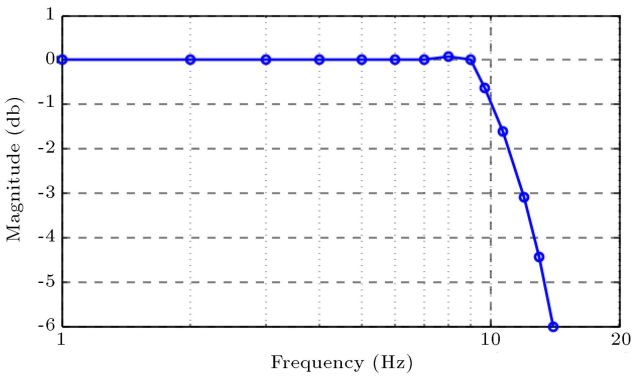

Figure 14. The frequency response diagram of the actuator obtained from experiments.

4.3.3. "Zero-resistance" control (back drivability experiment)

The most significant property of the elastic actuators is their ability to control the "zero-resistance" or back drivability amount. The control of "zero-resistance" is the lowest controllable amount of torque in the actuator output. This state is called the patient-based state in rehabilitation applications. In the patient-based state, patient walks freely, feeling no resistant torque from the actuator. The actuators in the engine-off state are automatically reversible; depending upon manufacturing type, friction, motor inertia etc., the back drivability is advantageous or disadvantageous.

In order to determine the actuator back drivability, first an interface arm, on which the force-gauge is installed, is connected to the actuator output. The system is shown in Figure 15. Then the force-gauge is connected to the interface arm. In this experiment, the same control loop of torque is used, but the torque input is considered to be zero (i.e. $M_{Ld} = 0$). With this control approach, with any torque applied at the output, the motion command is given to motor by the control loop in the torque direction. With this action, the person feels the lowest resistance at the output. The experiment is performed in two forms. First, the test is done while the engine is in the off-state. Then the motor is adjusted in the on-state and the

Figure 15. The force-gauge as well as the interface arm.

experiment is repeated. To perform the experiment, the force-gauge connected to the interface arm is took on hand and shaken. The amount of force required for the output movement is obtained by reading the indicated force. The amount of actuator resistance in output is determined by this experiment. The lower the value of obtained torque is, the lower the actuator resistance is in output. Now, by using Eq. (21), the value of torque at output can be obtained, where the length of the interface arm, d, is 0.2 m.

$$M_L = F_L * d. \tag{21}$$

Figure 16 shows the values of the force measured in the engine-off state. The value of the force found in the output is approximately 9 N. By substitution of the force in Eq. (21), the torque value is obtained to be $M_L = 1.8$ Nm. The forces measured by the force-gauge are in terms of STEP. Thus, to determine the experiment time, the time is measured manually by a time-keeper. The time for each experiment is shown below the relevant figure.

According to Figure 17, the recorded value of the force in the output is approximately 0.8 N. By substitution in Eq. (21), the torque value is obtained to be $M_L = 0.16$ Nm. Thus noting Figures 16 and 17, the measured value of torque at the output in the control-

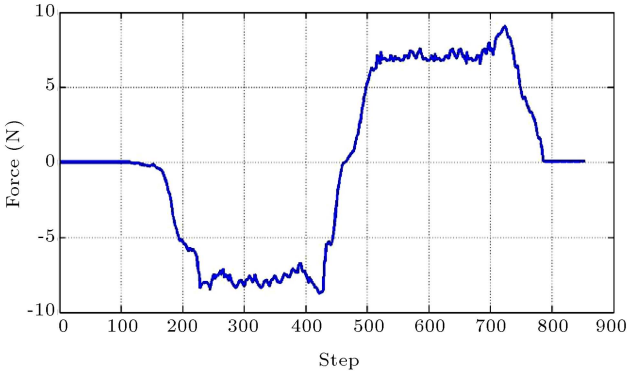

Figure 16. The force measured in the engine-off state in 1.7 sec.

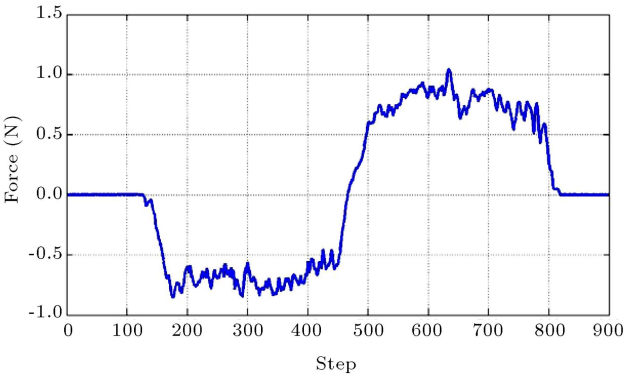

Figure 17. The force measured in the controlled (engine-on) state in 1.7 sec.

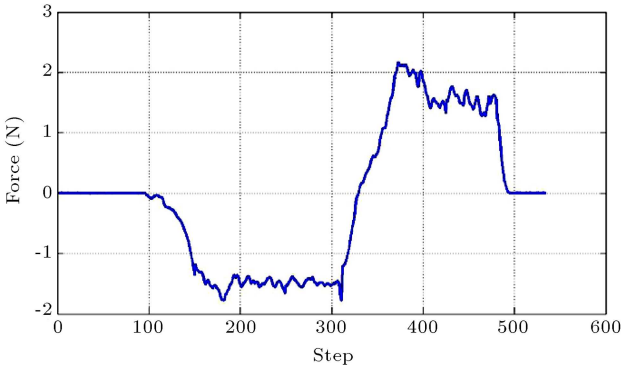

Figure 18. The force measured in the controlled (engine-on) state in 0.7 sec.

on state is approximately 10 percent of the torque value in control-off state. To test the actuator performance in higher frequencies, the experiment is repeated in lower duration of time (0.7 sec). Figure 18 shows the forces obtained by the force-gauge.

5. Conclusion

In the present paper, design, manufacturing and control of an elastic actuator are presented. The actuator is designed to meet the requirements of knee and hip joints of a rehabilitation robot. The speed feedback and PI controller are used for the actuator which results in many advantages for the actuator. A PID controller is used to control the output torque of the actuator. Implementation of the control algorithm and carrying out the considered tests, the following results are obtained.

5.1. Accuracy of torque measurement by spring

The significance of this experiment is due to the fact that the results of later experiments depend on the torque measurement by the spring. Besides, the more accurate the torque measurement by the spring is, the higher the actuator ability on performing the torque control commands will be. In Section 4.3.1, an appropriate and approximately linear behavior was shown by the spring, which is very significant for the actuator; because it means that the torque is measured with a high accuracy in the output.

5.2. Bandwidth of force-following with constant output

The actuator should have the ability to follow the required output torque of rehabilitation with high accuracy, so that it could be used in the rehabilitation applications. The results shown in previous section indicate that the actuator clearly follows the input torque. Thus, it can be concluded that the actuator can accurately follow required rehabilitation torques. In Figure 14, the Bode diagram for the bandwidth test

Table 6. The robot of the "Tarbiat Modares University" as well as the series elastic actuator.

Frequency (Hz)	Robot	Torque (Nm) engine-off state	Torque (Nm) engine-on state
0.6	TMU REHAB	1.8	0.16
	LOPES	5	1.5
1.4	TMU REHAB	3	0.4
	LOPES	10	4

of the actuator is shown. The actuator has a bandwidth of approximately 12 Hz. Due to the investigations of David Winter, the movement bandwidth for a healthy human-being is approximately 6 Hz [16]. Thus, the extensive bandwidth of the actuator shows that the designed actuator is very well capable of following the applied torques in frequency range of rehabilitation applications.

5.3. "Zero-resistance" control (back drivability experiment)

This test indicates the actuator back drivability in this control state. The results presented in Section 4.3.3 show that the actuator applies the lowest torque on the patient in control-appliance (engine-on) state when the actuator is in the patient-based state, in which the patient can freely move. The calculated value of torque in this state and in the frequency of 0.6 Hz is equal to 0.16 Nm. The measured value of torque is 10 percent of that of engine-off state. The results of this test show that the actuator has high ability for carrying out the impedance control, as in this test a model of the impedance control (zero-impedance) is carried out. To indicate efficiency of the actuator, the results obtained from this test are compared with the results presented for the actuator of the LOPES robot. The comparisons are demonstrated in Table 6. In this table, it can be seen that the LOPES robot gives a high torque in the engine-off state for the output displacement. However, the actuator offered in the present work has a lower torque compared to the actuator of LOPES robot. Thus, the designed actuator shows a much higher performance compared to that of LOPES robot. The advantages of the present actuator can also be observed in control-appliance state.

Due to the results from the experiments, it can be concluded that the actuator is able to accurately measure the torque generated at the output, and use this torque in the control loop. With these results, it can be said that the manufactured actuator has a high ability to carry out the required control states for rehabilitation. Due to these abilities, the actuator is used in manufacturing the rehabilitation robot of the "Tarbiat-Modarres University". Figure 19 shows how the actuator is used in robot of the "Tarbiat-Modarres University".

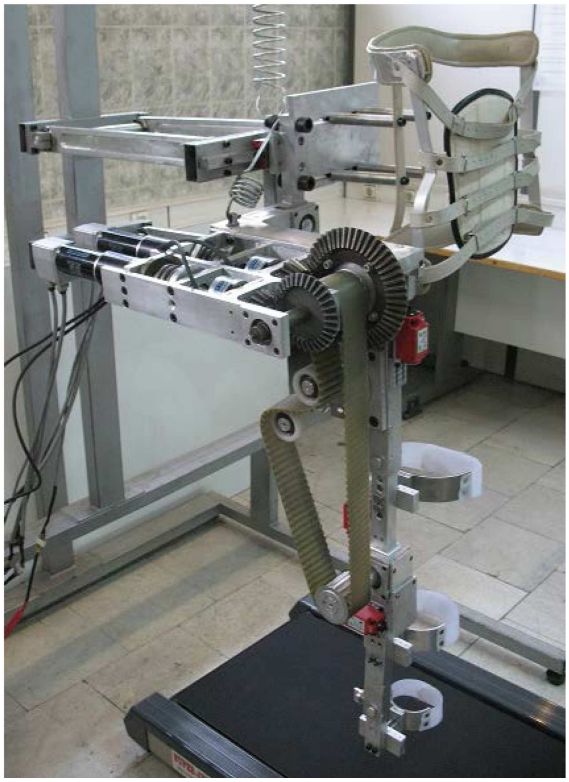

Figure 19. The robot of the "Tarbiat-Modarres University" as well as the series elastic actuator.

References

1. Robinson, D.W., Pratt, J.E., Paluska, D.J. and Pratt, G.A. "Series elastic actuator development for a biomimetic walking robot", *IEEE/ASME Int. Conf. on Advanced Intelligent Mechatronics*, pp. 561-568 (1999).

2. Kong, K., Bae, J. and Tomizuka, M. "A compact rotary series elastic actuator for knee joint assistive system", *IEEE Int. Conf. on Robot. Autom.*, pp. 2940, 2945 (2010)

3. Dollar, A.M. and Herr, H. "Lower extremity exoskeletons and active orthoses: Challenges and state-of-the-art", *IEEE Trans. on Robotics*, **24**(1), pp. 144,158 (2008).

4. Pratt, G.A. and Williamson, M.M. "Series elastic actuators", *IEEE/RSJ Int. Conf. on Intelligent Robot. Sys.*, **1**, pp. 399-406 (1995).

5. Garcia, E., Arevalo, J., Sanchez, F., Sarria, J. and Gonzalez-de Santos, P. "Design and development of

a biomimetic leg using hybrid actuators", In *Proc. IEEE/RSJ Int. Conf. Intell. Robot*, pp. 158-1512 (211).

6. Kong, K., Bae, J. and Tomizuka, M. "A compact rotary series elastic actuator for knee joint assistive system", *IEEE Int. Conf. Robot. Autom.*, pp. 2940-2945 (210).
7. Ragonesi, D., Agrawal, S., Sample, W. and Rahman, T. "Series elastic actuator control of a powered exoskeleton", *IEEE Annu. Int. Conf. Eng. Med. Biol. Soc.*, pp. 3515-3518 (211).
8. Sensinger, J.W. and Weir, R.F. "Unconstrained impedance control using a compact series elastic actuator", *IEEE/ASME 2nd Int. Conf. Mechatron. Embedd. Syst. Appl.*, pp. 1-6 (207).
9. Pratt, G., Willisson, P., Bolton, C. and Hofman, A. "Late motor processing in low-impedance robots: Impedance control of series-elastic actuators", *Amer. Control Conf.*, **4**, pp. 3245-3251 (2004).
10. Lagoda, C., Schouten, A., Stienen, A., Hekman, E. and van der Kooij, H. "Design of an electric series elastic actuated joint for robotic gait rehabilitation training", *IEEE 3rd RAS and EMBS Int. Conf. Biomed. Robot. Biomechatron.*, pp. 21-26 (210).
11. Thorson, I. and Caldwell, D. "A nonlinear series elastic actuator for highly dynamic motions", *IEEE/RSJ Int. Conf. Intell. Robot.*, pp. 390-394 (211).
12. Vallery, H., Ekkelenkamp, R., van der Kooij, H. and Buss, M. "Passive and accurate torque control of series elastic actuators", *IEEE/RSJ Int. Conf. Intell. Robot.*, pp. 3534-3538 (208).
13. Wyeth, G. "Control issues for velocity sourced series elastic actuators", *Australasian Conf. Robot. Autom.*, Mill Valley, CA (1989).
14. Hurst, J., Chestnutt, J. and Rizzi, A. "The actuator with mechanically adjustable series compliance", *IEEE Trans. Robot.*, **26**(4), pp. 597-67 (210).
15. Hurst, J., Rizzi, A. and Hobbelen, D. "Series elastic actuation: Potential and pitfalls", *Int. Conf. Climb. Walk. Robot.* (2004).
16. Winter, D.A., *Biomechanics and Motor Control of Human Movement*, John Wiley & Sons (1990).

Biographies

Mohammad Davoodi Hasankola was born in Babol, Iran, in 1986. He received his MS degree in Mechanical Engineering from Tarbiat Modares University, Tehran, Iran, in 2012. His MS thesis focuses on elastic actuator for rehabilitation robots. His research interests are elastic actuator and rehabilitation robotics.

Abbas Ehsaniseresht was born in Tehran, Iran, in 1983. He received his PhD degree in Mechanical Engineering from Tarbiat Modares University, Tehran, Iran, in 2014. His PhD thesis focuses on patient-centered gait training using robotic orthosis. Since 2014 he has been working as a professor assistant in Mechanical Engineering at Hakim Sabzevari University, Sabzevar, Iran. His research interests are rehabilitation robotics and control systems.

Majid Mohammadi Moghadam Received the BSc degree in Mechanical Engineering in 1988, from Sharif University of Technology, Iran, and MEng degree in Mechanical Engineering, in 1993, from McGill University, Canada, and PhD degree in Mechanical Engineering, in 1996, from University of Toronto, Canada. He is Professor of Mechanical Engineering at Tarbiat Modares University, Tehran, Iran. His current research, which focuses on applied robotics and robust H^{∞} control, is concerned with haptic robotics, rehabilitation robotics, inspection robotics and rough terrain mobile robot design. He is a member of the Administrative Committee of Robotics and Mechatronics Societies of Iran. He has served as Co-Chair for many national /international conferences in Iran.

Ali Akbar Mirzaei Saba was born in Bahar, Iran, in 1986. He received his MS degree in mechanical engineering from Tarbiat Modares University, Tehran, Iran, in 2012. His MS thesis focuses on Mechanism of rehabilitation robots. His research interests are rehabilitation robotics and control systems.